

Exploring Seawater Oxidation Potential with MnCoCr Layered Double Hydroxides @ Sulphur Doped Carbon Dots/Nickel foam Electro catalyst in an Alkaline Environment

Mahalakshmi Vedanarayanan^a, Chandrasekaran Pitchai^b and Sethuraman Mathur Gopalakrishnan ^{a*}

^a Department of Chemistry, The Gandhigram Rural Institute (Deemed to be University), Gandhigram, Dindigul, TN, India – 624 302.

^b Department of Chemical Engineering, National Chung Hsing University, Taichung 402, Taiwan.

Email: mgsethu@gmail.com

Materials

Cobalt nitrate hexahydrate ($\text{Co}(\text{NO}_3)_3 \cdot 6\text{H}_2\text{O}$), Manganese nitrate tetrahydrate ($\text{Mn}(\text{NO}_3)_3 \cdot 4\text{H}_2\text{O}$), Chromium nitrate nonahydrate ($\text{Cr}(\text{NO}_3)_3 \cdot 9\text{H}_2\text{O}$), urea ($\text{CO}(\text{NH}_2)_2$), sodium carbonate (Na_2CO_3), potassium hydroxide (KOH) and sodium hydroxide (NaOH) were purchased from Sisco Research Laboratories (SRL). The prawn shells and the sea water were collected from the coastal region of Bay of Bengal near Poompuhar. Double distilled water (DD) was used throughout the study both for synthesizing the material and preparing electrolytic solution. Nickel Foam (NF), platinum (Pt) wire electrode and silver/silver chloride (Ag/AgCl) electrode were purchased from Sinsil International Pvt. Ltd., Bengaluru, India.

Preparation of alkaline sea water

For the preparation of 1M KOH solution using sea water, at first sea water was processed for removing precipitates like $\text{Mg}(\text{OH})_2$ and $\text{Ca}(\text{OH})_2$. So, 1 M Na_2CO_3 was added to 250 mL of sea water to precipitate Mg^{2+} and Ca^{2+} ions effectively. Due to this precipitation, it reduced the risk of blockage of the active sites on the working electrode during HER and OER. After precipitation, the electrolytic solution was filtered and used for the electrochemical reaction.

Corrosion resistance of the material

The mechanism underlying the corrosion resistance of the catalyst was intricate, especially concerning the properties of MnCoCr LDH@SCDs. MnCoCr LDH comprised layers of metal hydroxides composed of Mn, Co, and Cr, carrying positive charges of 2+, 3+, and 4+, respectively, interspersed with negatively charged species such as carbonate or nitrate ions. The specific composition of MnCoCr LDH influenced its ability to resist corrosion in seawater. The layered structure not only acted as a physical barrier against the infiltration of corrosive elements but also repelled anions present in seawater, thereby impeding the entry of corrosive substances. Furthermore, MnCoCr LDH could form passive layers on its surface when exposed to seawater, serving as a shield against further corrosion. This passivation process involved the formation of insoluble metal oxide/hydroxide layers on the LDH surface, effectively reducing the corrosion rate. The passive layer acted as both a physical and chemical barrier, preventing additional corrosion of the LDH electrode. Additionally, the nickel foam substrate was densely coated with LDH species, demonstrating an anti-corrosion approach involving the intercalation of high-valence anions in LDH. In this strategy, the presence of high-negatively charged anions within the interlayers hindered the corrosion of the Ni substrate through electrostatic repulsion. Furthermore, the use of inert protective layers, such as sulfur-doped carbon dots (SCDs), helped to protect the active material from corrosion induced by chloride ions (Cl^-) while enhancing electrical conductivity. As a result, the pairing of MnCoCrV LDH and SCDs effectively mitigated corrosion in seawater.

Characterization of MnCoCr LDH@SCDs, MnCoCr LDH and SCDs

As-prepared samples (MnCoCr LDH@SCDs, MnCoCr LDH and SCDs) were studied by EDX, XRD, FT-IR, SEM, HR-TEM and XPS for structural change and elemental composition. The SEM and HR-TEM were applied for analyzing the morphological changes which obtained from VEGA3, TESCAN (Czech Republic) and FEI Technai G220 S-TWIN HR-TEM operating at 200 Hz respectively. The X-ray diffraction (XRD) of the resulting samples were investigated by using $\text{Cu K}\alpha$ radiation with the wavelength of 1.54 Å from PANalytical X'Pert diffractometer. By BRUKER

Nano, GmbH, D-12489 Energy dispersive X-ray spectroscopy, the elements present and its composition were determined. Metals electronic states and the functional groups present were obtained by the use of XPS and Jasco FT- IR 460 Plus analyzer (PHI 5000 Versa Probe II), respectively.

Electrochemical studies

The electrochemical properties of MnCoCr LDH@SCDs, MnCoCr LDH, and SCDs materials were investigated in a standard three-electrode system using a CHI 760 D work station in a pH 14 alkaline medium of 1 M KOH. The nickel foam (NF) surface was coated with these synthesized materials and used as the working electrode, while the Ag/AgCl electrode and Pt wire electrode served as the reference and counter electrodes, respectively. To prepare the NF, it was first cut into 1x1 cm² pieces, sonicated in acetone and 3 M HCl for 20 minutes, washed with DD water and ethanol, and dried thoroughly. The synthesized materials were then dropcast onto the NF, resulting in MnCoCr LDH@SCDs/NF, MnCoCr LDH/NF, and SCDs/NF. To dropcast the materials, 10 mg of the required material was mixed with 20 μL of 5% nafion and ethanol/water, and then dried and utilized as the working electrode. To compare their electrocatalytic behaviour, we also dropcasted the benchmark RuO₂/NF. Prior to running the electrochemical studies, such as OER, we purged the electrolyte with oxygen for 30 minutes.

Determining the kinetics of a reaction is significantly influenced by the application of overpotential. Linear sweep voltammetry (LSV) was carried out at a scan rate of 10 mV/sec to measure without compensating for iR, where "i" denotes the tested current and "R" represents the difference in resistance between the working and reference electrodes. The reference potential used was the reversible hydrogen electrode (RHE), and the potentials obtained from the working electrode were converted to RHE potential using Eqn. 1.

$$E_{RHE} = E_{WE} + 0.0591 \times pH + E_{Ag/AgCl} (ref) \dots\dots\dots (1)$$

This equation considers the potentials of the working electrode (EWE) and the Ag/AgCl electrode (EAg/AgCl). The overpotentials (η) at the current density of 10 mA/cm² were then determined using Eqn. 2, which involved subtracting the RHE potential from 1.23 V.

$$\eta = E_{RHE} - 1.23 \text{ V} \dots\dots\dots (2)$$

To examine the long-term stability of the synthesized materials, chronopotentiometry was performed at a constant current density of 10 mA/cm² for about 24 hours.

The electrochemical active surface area (ECSA) was measured to confirm the high activity of the material, using cyclic voltammetry (CV) at different scan rates of 10, 20, 30, 50, 75, and 100 mV/s within the desired frequency range. The ECSA was calculated from the CV curves using Eqn. 3, which considered the double layer capacitance (C_{dl}) and specific capacitance (C_s).

$$\text{ECSA} = C_{dl}/C_s \quad \dots\dots\dots (3)$$

Finally, to determine the greater conductivity of the synthesized material, electrochemical impedance spectroscopy (EIS) was performed at open circuit potential from the frequency of 10⁴ to 1.0 Hz with 5 mV amplitude, which allowed for the measurement of the charge-transfer resistance.

Faradic Efficiency

The quantity of measured gas was determined by accumulating the generated oxygen, assuming a constant generation rate during each 500 s period. The ideal O₂ production (assuming 100% Faradaic efficiency) was calculated using the following relationship.

$$10 \text{ mA} = 10 \text{ mC/s} = (10^{-2} \text{ C/s}) / (96485 \text{ C/eq} \times 4 \text{ eq/mol}) = 2.591 \times 10^{-8} \text{ mol/s}$$

The volumetric fraction of evolved oxygen is subsequently calculated using the ideal gas law, which is then compared to the standard peak (the oxygen peak of fresh air). Faradaic efficiency is determined by dividing the measured generation rate by the theoretical generation rate.

$$\text{Faradic Efficiency (FE)} = [\text{Measured (actual) generation} / \text{Theoretical (calculated) generation}] \times 100\%$$

UV-Visible spectroscopy

The UV-Visible spectroscopy can be employed to analyze the optical characteristics of synthesized SCDs. In Figure S5, the UV-Visible spectrum reveals two distinctive shoulders at 270 and 330 nm, corresponding to π - π^* and n- π^* electronic transitions. These transitions confirm the presence of sp² carbon (C=C) and carbonyl groups in the carbon dots.

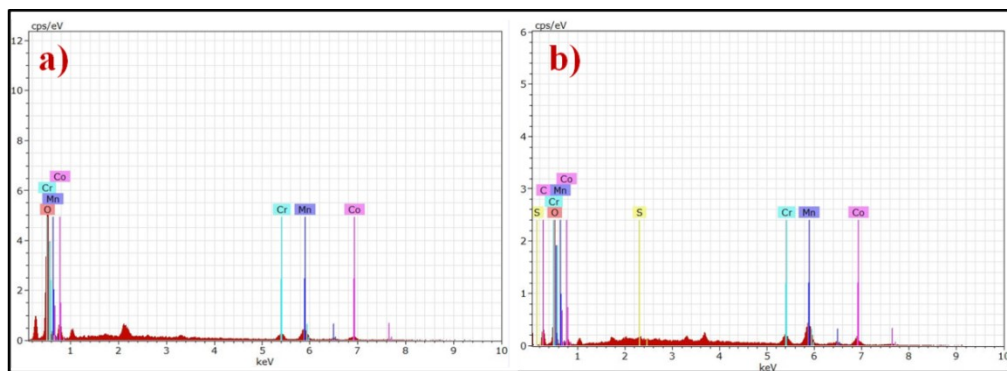


Fig.S1 EDX spectra of a) MnCoCr LDH and b) MnCoCr LDH@SCDs

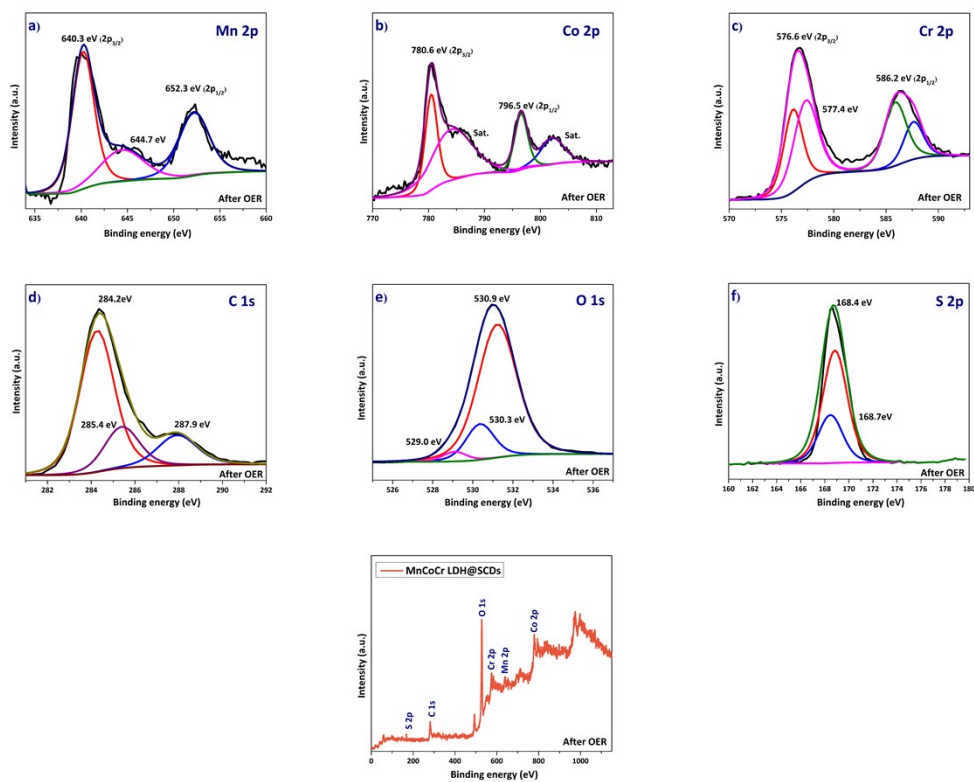


Fig.S2 XPS survey spectra of MnCoCr LDH@SCDs after OER

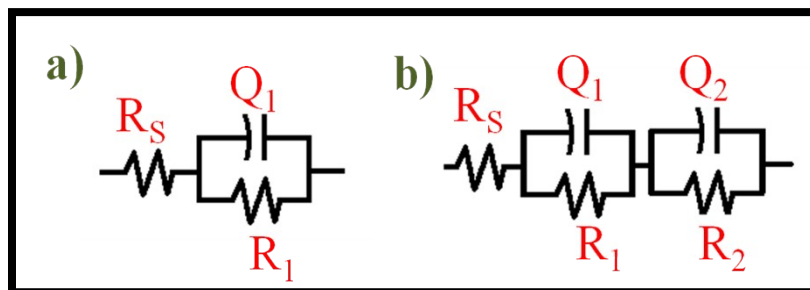


Fig.S3 Equivalent fitted circuit for (a) bare NF and (b) MnCoCr LDH and MnCoCr LDH@SCDs

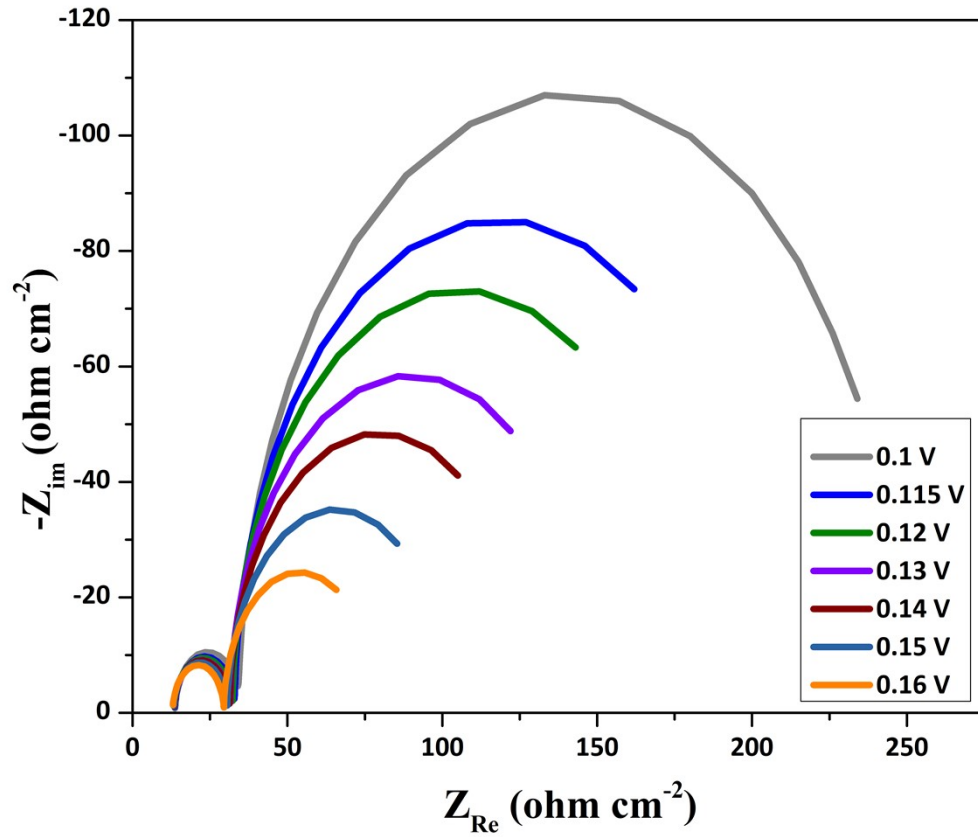


Fig.S4 Nyquist plots for MnCoCr LDH@SCDs at different OER potentials

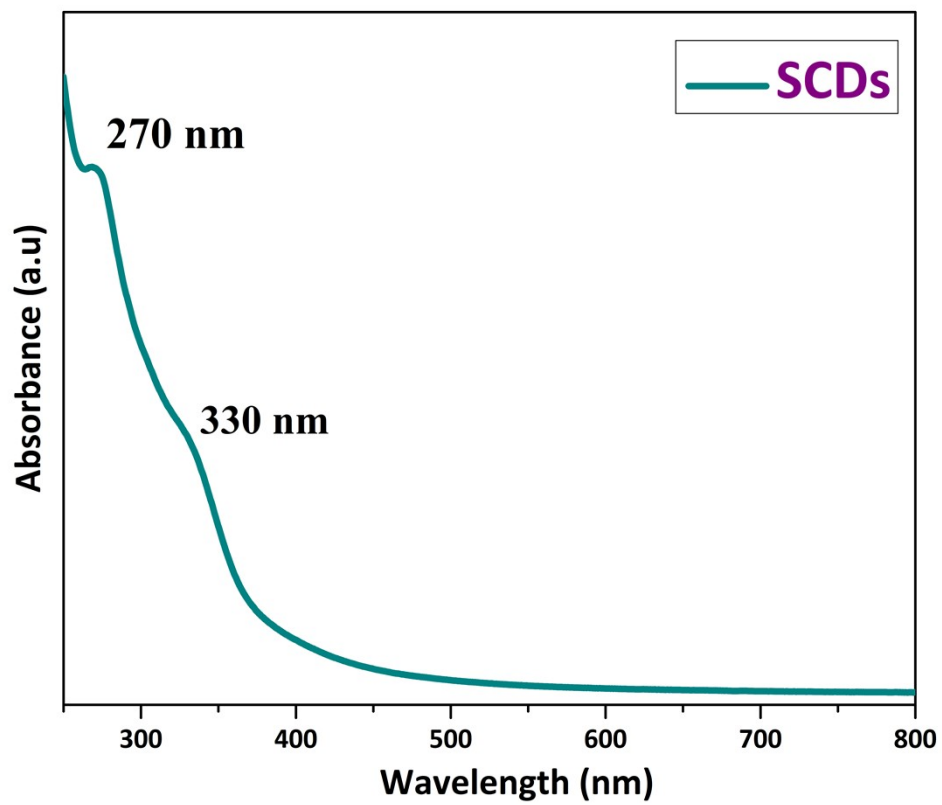


Fig.S5 UV-Visible spectrum of SCDs

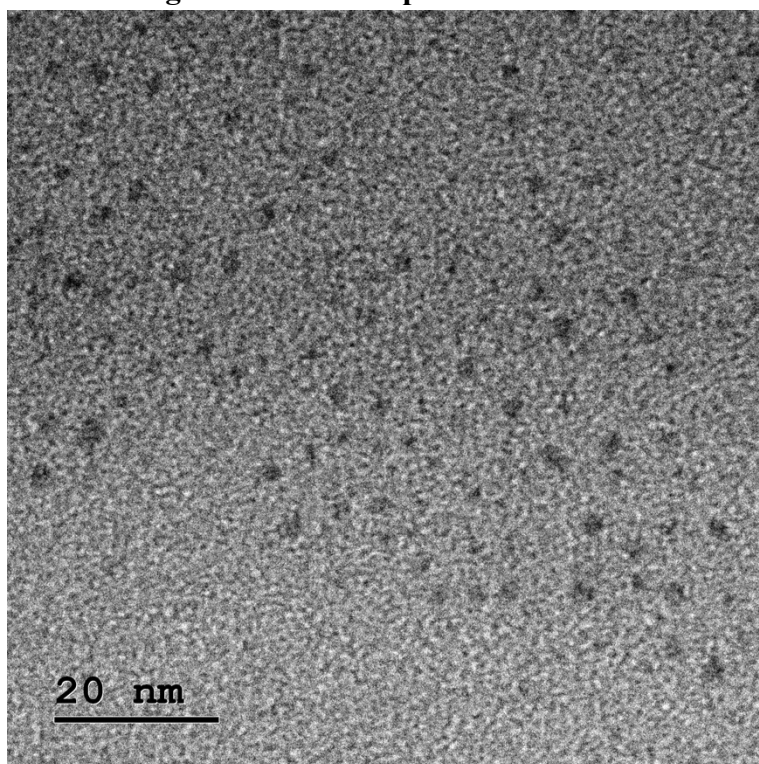


Fig.S6 HR-TEM image of SCDs

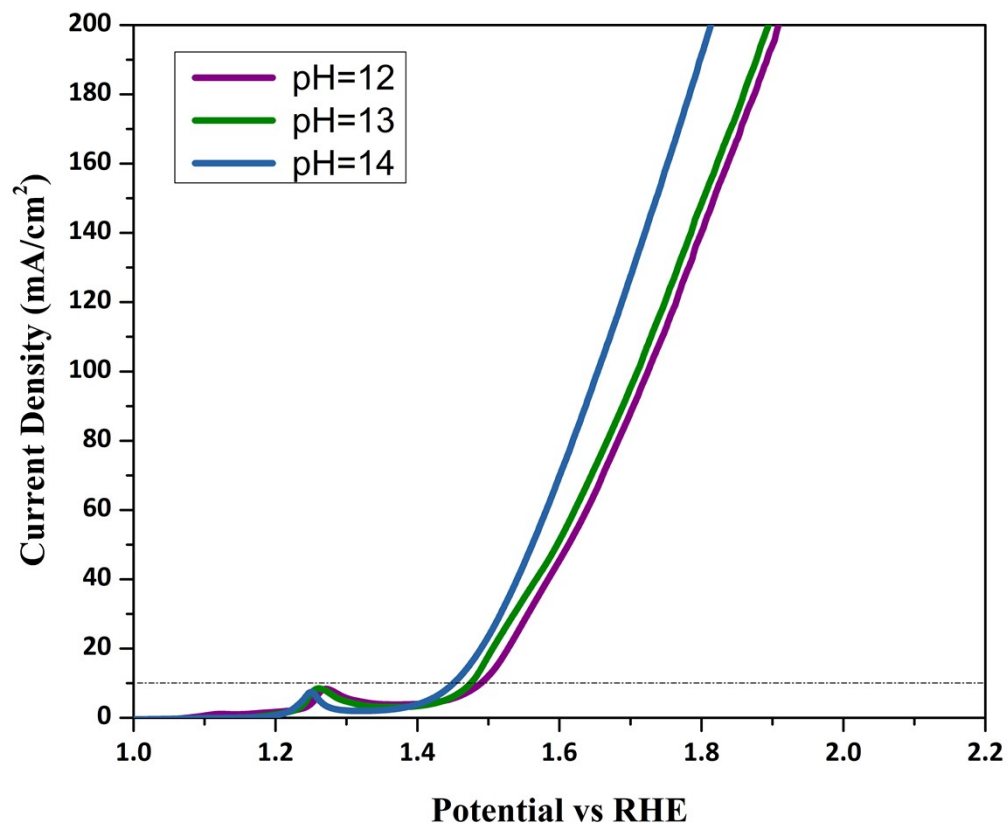


Fig.S7 LSV curves at different pH conditions